

VU Research Portal

Overwintering fires in boreal forests

Scholten, Rebecca C.; Jandt, Randi; Miller, Eric A.; Rogers, Brendan M.; Veraverbeke, Sander

published in

Nature
2021

DOI (link to publisher)

[10.1038/s41586-021-03437-y](https://doi.org/10.1038/s41586-021-03437-y)

document version

Peer reviewed version

document license

Other

[Link to publication in VU Research Portal](#)

citation for published version (APA)

Scholten, R. C., Jandt, R., Miller, E. A., Rogers, B. M., & Veraverbeke, S. (2021). Overwintering fires in boreal forests. *Nature*, 593(7859), 399-404. <https://doi.org/10.1038/s41586-021-03437-y>

General rights

Copyright and moral rights for the publications made accessible in the public portal are retained by the authors and/or other copyright owners and it is a condition of accessing publications that users recognise and abide by the legal requirements associated with these rights.

- Users may download and print one copy of any publication from the public portal for the purpose of private study or research.
- You may not further distribute the material or use it for any profit-making activity or commercial gain
- You may freely distribute the URL identifying the publication in the public portal ?

Take down policy

If you believe that this document breaches copyright please contact us providing details, and we will remove access to the work immediately and investigate your claim.

E-mail address:

vuresearchportal.ub@vu.nl

2 **Article citation:** Scholten, R.C., Jandt, R., Miller, E.A. *et al.* Overwintering fires in boreal
3 forests. *Nature* **593**, 399–404 (2021). <https://doi.org/10.1038/s41586-021-03437-y>

4 **Overwintering fires in boreal forests**

5 Rebecca C. Scholten^{1*}, Randi Jandt², Eric A. Miller³, Brendan M. Rogers⁴ and Sander
6 Veraverbeke¹

7 ¹ Faculty of Science, Vrije Universiteit Amsterdam, 1081 HV Amsterdam, North Holland, The
8 Netherlands.

9 ² Alaska Fire Science Consortium, University of Alaska, Fairbanks, AK, USA.

10 ³ Bureau of Land Management, Alaska Fire Service, Fort Wainwright, AK 99703, USA.

11 ⁴ Woodwell Climate Research Center, Falmouth, MA, USA.

12 *Correspondence to: r.c.scholten@vu.nl.

13
14 **Forest fires are usually viewed within the context of a single fire season, in which weather**
15 **conditions and fuel supply can combine to create conditions favourable for fire ignition –**
16 **usually from lightning or human activity – and spread^{1–3}. But some fires exhibit**
17 **overwintering behaviour, in which fires smoulder through the non-fire season and flare-up**
18 **in the subsequent spring^{4,5}. Boreal forests, with deep organic soils favourable for**
19 **smouldering⁶ and accelerated climate warming⁷ may present unusually favourable**
20 **conditions for overwintering. Still, the extent of overwintering in boreal forests and the**

21 **underlying factors influencing overwintering behaviour remain unclear. Here we show that**
22 **overwintering fires in boreal forests are associated with hot summers generating large fire**
23 **years and deep burning into organic soils, conditions that have become more frequent in our**
24 **study areas in recent decades. Our results are based on an algorithm to detect overwintering**
25 **fires in Alaska, USA, and Northwest Territories, Canada, using field and remote sensing**
26 **datasets. Between 2002 and 2018, overwintering fires were responsible for 0.8 % of the total**
27 **burned area; however, in one year this amounted to 38 %. The spatiotemporal predictability**
28 **of overwintering fires could be leveraged by fire management agencies to facilitate early**
29 **detection, which may result in reduced carbon emissions and firefighting costs.**

30 Arctic-boreal regions are warming faster than the global average^{7,8}, and are estimated to store more
31 than twice as much carbon as the Earth's atmosphere in their organic soils⁹. Fires are a natural
32 disturbance in boreal forests and release carbon from above- and belowground carbon pools into
33 the atmosphere. A large fraction of the carbon emissions from fires in northern high latitudes
34 originates from belowground carbon pools as these fires often burn deep into organic soils¹⁰⁻¹². In
35 a warming climate, boreal fire regimes are intensifying and fires may burn deeper into organic
36 soils and thereby threaten soil carbon reservoirs^{10,13}. Moreover, increasing summer temperatures
37 in northern high latitudes lead to more severe fire weather¹⁴ and more lightning ignitions² that
38 enable fires to burn more area, although regional differences in decadal burned area trends exist
39 and the relatively short length of consistent burned area time series influences the interpretation¹⁵.
40 Containment expenses increase exponentially with fire size, and therefore large fires constitute the
41 majority of the budget allocated to fire management agencies in the USA and Canada^{16,17}. The
42 stagnant fire management budgets¹⁸ in the USA and Canada are under pressure because of the
43 increasing threats of climate warming and continued expansion of dwellings into the wildland

44 urban interface. Prevention and aggressive initial attack on undesired fires may be a viable way to
45 lower firefighting costs^{16,18}.

46 Traditionally, the fire season in high latitudes begins with the lightning season in June or early-
47 season human activities like debris burning^{2,3,19}. Once ignited, boreal fires can smoulder in organic
48 soils during periods when weather does not favour flaming spread, and, after days or months, re-
49 emerge under weather conditions that favour flaming^{1,20,21}. Smouldering boreal fires often remain
50 undetected, especially in remote areas, which poses challenges for fire managers¹. Recently, fire
51 managers in Alaska, USA, and the Northwest Territories, Canada, started reporting an increasing
52 number of extreme manifestations of this holdover phenomenon. In such cases, some fires
53 hibernate in deep organic soil layers for seven to eight months during the winter and re-emerge
54 early the next fire season, in what can appear to be a new ignition. Limited and often anecdotal
55 evidence of these overwintering fires exists in recent Alaskan fire management reports and
56 operating plans^{22,23}, as well as news reports²⁴. Overwintering, or “zombie” fires, are an
57 understudied phenomenon in boreal forests and may have severe implications for fire management,
58 human health, and climate^{4,5}.

59 **Detection of large overwintering fires**

60 Overwintering fires typically undergo four temporal stages. Towards the end of a fire season, the
61 fire seemingly stops burning as flaming spread ceases (Fig. 1A). Unnoticed, it smoulders during
62 winter under the snow cover (Fig. 1B). As soon as fire weather facilitates fire spread the following
63 fire season, the fire flames up (Fig. 1C, Extended Data Fig. 1), thereby burning additional area
64 (Fig. 1D). This sequence of events allows for the identification of spatial and temporal
65 characteristics of overwintering fires. First, newly burned areas of an overwintering fire are found

66 near the original burn scar, and second, they require no additional ignition source and can therefore
67 re-emerge early in the fire season, before the main lightning season.

68 We developed an algorithm to retrospectively identify and map overwintering fires based on these
69 two spatiotemporal characteristics (Extended Data Fig. 2). We analysed the locations of 45 small
70 overwintering fires reported by fire managers in Alaska and the Northwest Territories between
71 2005 and 2017 to determine a suitable threshold for the distance between a holdover and its fire of
72 origin. With small fires we refer to fires whose re-emergence remained undetected in the Moderate
73 Resolution Imaging Spectroradiometer (MODIS) active fire product²⁵. Small overwintering fire
74 sizes ranged from 0.04 to 42.5 ha, and 78 % of the fires burned less than 1 ha. We found that 89 %
75 of these small overwintering fires started within the fire perimeter from the year before, and 93 %
76 travelled less than 500 m over the winter (Extended Data Fig. 3). Our results are consistent with
77 laboratory experiments on boreal peat, which have shown that smouldering fires spread around
78 100 - 250 m/yr (10 - 30 mm/h) depending on oxygen supply and water and mineral contents of the
79 peat⁶. We therefore adopted a threshold of 1000 m to search for overwintering flare-ups in the
80 vicinity of burned area from the year before. The 1000 m threshold was chosen because it is the
81 approximate nadir pixel size of the MODIS active fire product that we used to detect fires.

82 In Alaska and Northwest Territories, fine fuels are conducive to flaming spread as early as mid- to
83 late May, even before convective thunderstorm activity starts²⁶. The timing of dry fuel availability
84 is dependent on the onset of snowmelt in spring, which varies in time and space²³. Spring snow
85 melt is dependent on winter and spring temperatures and precipitation and therefore a suitable
86 proxy of spring and winter weather conditions, and has been shown to be an effective predictor of
87 fire activity²⁷. To capture the annual variability in dry fuel availability, we based the temporal
88 constraint of our algorithm on the regional yearly snowmelt day, which we calculated from the

89 MODIS daily fractional snow cover product (MODSCAG)²⁸. We analysed the difference between
90 the regional snowmelt day and the detection dates of the 45 reported overwintering fires, and found
91 that overwintering fires re-emerged on average 27 days (standard deviation: 18.5 days) after the
92 regional snowmelt onset. Regionally, overwintering fires on average re-emerged at the end of May
93 (Julian day: 150, standard deviation: 17.9 days). We therefore used the 90th percentile of 48 days
94 after the regional snowmelt onset as the temporal threshold within the detection algorithm for
95 overwintering fires. Since the satellite product detects fires on average two days later than fire
96 managers, we increased the temporal threshold to a total of 50 days. Lastly, in addition to the
97 spatial and temporal constraints, our algorithm eliminated fires that started close to human
98 infrastructure or close in space and time to a recorded lightning strike (Extended Data Fig. 4).
99 Excluding areas close to infrastructure means some overwintering fires may be missed, but
100 eliminates a larger number of false positives from spring pile burning and other anthropogenic
101 influences around settlements.

102 In addition to the 45 small reported overwintering fires, which we used for algorithm development,
103 we used a subset of nine larger overwintering fires (mean size: 20312, standard deviation: 24185
104 ha), which were large enough to be detected by the MODIS active fire product, as validation data
105 for our algorithm (Supplementary Table 1). We extracted the re-emergence date and distance to
106 burn scars of the antecedent year for all ignitions from the Alaskan Fire Emissions Database
107 (AKFED)²⁹, and applied our detection algorithm to them. We detected seven out of nine of the
108 large field-verified overwintering fires.

109 Furthermore, we identified 20 previously unreported large overwintering fires in Alaska and the
110 Northwest Territories between 2002 and 2018 (Supplementary Table 2). Large overwintering fires
111 constitute 0.8 % of the total burned area and 0.5 % of the total carbon emissions, yet their relative

112 contribution can be substantial in individual years and amounted to more than 5 % in three years
113 in Alaska (2007, 2008 and 2010) and two years in the Northwest Territories (2002 and 2015). For
114 example, in Alaska in 2008, the contribution of a single overwintering fire that burned 13700 ha
115 amounted to 38 % of the annual burned area.

116 **Temporal drivers of overwintering fires**

117 Years with large annual burned area more frequently produced overwintering fires (Fig. 2). Fire
118 season temperature and annual burned area were strongly correlated for both Interior Alaska
119 (Extended Data Fig. 5, Spearman's $\rho = 0.59$, $p < 0.001$) and the Northwest Territories ($\rho = 0.41$,
120 $p = 0.097$), and we found increasing temperature trends in both areas, and in burned area for
121 Interior Alaska (Fig. 2). Temperature trends differed within regions and the largest warming was
122 observed in western Interior Alaska and central Northwest Territories (Extended Data Fig. 5).
123 Fire season temperature and burned area correlated strongly with the number of overwintering
124 fires in both regions (Fig. 2, Extended Data Fig. 6). Several fires of the large fire years 2009 and
125 2015 in Alaska and the extreme 2014 fire season in the Northwest Territories overwintered.
126 While burned area in the antecedent year is prerequisite for the occurrence of overwintering
127 fires, we found that fires survived winter following the six hottest summers in the Northwest
128 Territories, whereas overwintering was not observed after the seven coolest summers. Our results
129 based on average fire season temperature are further supported by an analysis that focused on
130 extreme temperatures (Extended Data Figure 7). We found that the number of hot days that
131 surpassed the longer-term 90th percentile of daily maximum temperature during the fire season
132 correlated strongly with annual burned area (Alaska: $\rho = 0.71$, $p < 0.001$; Northwest Territories:
133 $\rho = 0.50$, $p = 0.001$), and with the number of fires that overwintered. Large scale climatic drivers
134 thus govern the survival and growth of overwintering fires. In autumn, fires in boreal regions are

135 usually extinguished by substantial rain events¹. Extended fire seasons and droughts associated
136 with climate warming^{30,31} may counteract the natural fire extinction in autumn and instead
137 increase the chances of fires entering a smouldering phase. An important driver modulating the
138 emergence of large overwintering fires may therefore be warm and extreme summers that
139 facilitate long and large fire seasons^{31,32}. Within our time series, we found no evidence that
140 winter and spring meteorology or the snowmelt timing influence the survival of large
141 overwintering fires (Extended Data Tables 1 and 2).

142 Our reference data on overwintering fires contained five times as many small fires that were
143 undetected by satellite imagery, as large, detected fires, suggesting that, when re-emerging in
144 spring, these fires usually remain relatively small and undetected, and only occasionally grow
145 large when fire weather conditions favour fire spread. Large overwintering fires on average
146 experienced more severe fire weather at the time of the flare-up than small overwintering fires
147 (Extended Data Table 3), yet this relationship may partly be confounded by interacting effects of
148 fire spread direction and limited fuel availability in the burned area of the antecedent year.

149 **Spatial drivers of overwintering fires**

150 For a fire to overwinter it needs to burn deep into the organic soil or underneath tree roots so that
151 the organic soil can protect and insulate from adverse winter conditions³³. Severe fires burn deep
152 into the soil organic layers³⁴ and may thus help sustain the smouldering phase of overwintering
153 fires during winter. We analysed burn depth data from AKFED, and found that, on average, fires
154 that promoted overwintering had burned deeper into the organic soil layer than those that stopped
155 burning at the end of the fire season for both Alaska (14.0 cm vs. 12.6 cm, $p = 0.07$) and the
156 Northwest Territories (16.7 cm vs. 14.1 cm, $p = 0.02$) (Fig. 3, Table 1), indicating that deep
157 burning may facilitate overwintering of fires. Regionally, burn depth is correlated with the 90th

158 percentile of daily maximum temperature in summer in both regions (Extended Data Fig. 7,
159 Alaska: $\rho = 0.56$, $p = 0.02$, Northwest Territories: $\rho = 0.48$, $p = 0.047$). Extreme temperatures
160 have increased since 1979 in western Interior Alaska and central and southern Northwest
161 Territories (Extended Data Fig. 5).

162 Burn depth in organic layers is co-influenced by fire weather, topographic landscape position and
163 vegetation and soil characteristics^{11,12,35,36}. We compared topographic indicators, pre-fire tree
164 cover and tree species dominance, and carbon in the organic soil layer of fires that produced
165 overwintering fires to those that did not facilitate overwintering (Table 1). Overwintering fires
166 were associated with flat, low-elevation areas, both in Alaska and the Northwest Territories (Fig.
167 4, Table 1). Lowland terrain in Alaska and the Northwest Territories typically features thick
168 organic soil. Indeed, overwintering fires occur more often in areas with higher carbon contents in
169 the upper soil layer (0 - 30 cm) in Alaska ($p = 0.003$), however, this driver was not significant in
170 the Northwest Territories. Tree cover and species modulate fire severity by their influence on
171 fuel availability and connectivity³⁷. We found that fires that produced overwintering fires have a
172 higher tree cover ($p = 0.001$) and a larger fraction of black spruce ($p = 0.09$) in Alaska, yet these
173 drivers were not significant in the Northwest Territories. Fires occur in more varied landscapes
174 with regard to soil carbon content and forest composition in Alaska compared to the Northwest
175 Territories (Table 1), which may explain why some of these drivers were significant in Alaska
176 but not in the Northwest Territories.

177 **Climate change and fire management**

178 We identified three main drivers of overwintering fires that are influenced directly by climate
179 warming: summer temperature extremes, large annual fire extent and deep burning. Higher
180 temperatures in boreal regions lead to intensified drought and elongated fire seasons³². Longer

181 fire seasons allow fires to spread faster and grow larger, thereby leading to large area burned³⁸.
182 Summer heat and drought induce deep drying of surface organic fuels, and are thus associated
183 with higher fire severity and deep burning¹². Increasing summer temperatures associated with
184 climate warming may thus promote the survival of overwintering fires in the future. Likewise,
185 earlier onset of spring fire weather conditions may lead to a larger fraction of these fires growing
186 large. At the same time, ecosystem shifts towards a dominance of deciduous vegetation due to
187 increasing fire severity³⁹ and higher temperatures⁴⁰ may constrain the occurrence of
188 overwintering fires in the future. Hence, the fate of overwintering fires in the changing boreal
189 biome will depend on counteracting processes that facilitate or constrain their occurrence.

190 Overwintering fires are currently a relatively rare phenomenon in boreal forests. Yet, because of
191 their long duration and extended smouldering phase, overwintering fires may substantially
192 influence soil functioning and post-fire recovery trajectories³⁴. We estimated that large
193 overwintering fires in Alaska and the Northwest Territories emitted 3.5 (standard deviation: 1.1)
194 Tg carbon between 2002 and 2018, 64 % of which occurred during the 2015 NWT and 2010
195 Alaska fire seasons. The contribution of smouldering combustion is generally underestimated in
196 carbon emission estimates from boreal fires²⁰. Thus, our estimate is likely conservative, since
197 overwintering fires exhibit a substantial smouldering phase and may burn deeper than our
198 emissions model currently predicts. In addition, smouldering fires emit relatively more methane
199 and less carbon dioxide in comparison to flaming fires⁴¹, yet methane has a much larger global
200 warming potential⁴².

201 Carbon emissions from overwintering fires currently contribute 0.5 % of the total carbon
202 emissions from fires in Alaska and Northwest Territories, yet this fraction may grow larger with
203 climate warming. We have shown that overwintering fires have temporal and spatial

204 predictability. Space- and airborne monitoring of the edges of burn scars from the preceding year
205 in lowland forested peatlands early in the fire season, and especially after a year with large
206 burned area, may prove beneficial for detecting and suppressing flare-ups from overwintering
207 fires while they are small. Fire suppression has shown to be most successful and cost-effective
208 when applied early and on small fires^{16,17}. Out of the 26 overwintering fires for which we had
209 suppression cost data in Alaska, the single largest fire caused 80 % (\$2.2 million) of the total
210 costs incurred by all overwintering fires (Supplementary Tables 1 and 2). Early detection and
211 attack on overwintering fires could thus contribute to savings in the fire management budget that
212 is under increasing pressure¹⁸. In addition, targeted monitoring and early suppression of
213 overwintering fires could help fire managers preserve terrestrial carbon stores when suppression
214 is part of a climate change mitigation strategy.

215 **References:**

- 216 1. Sedano, F. & Randerson, J. T. Multi-scale influence of vapor pressure deficit on fire
217 ignition and spread in boreal forest ecosystems. *Biogeosciences* **11**, 3739–3755 (2014).
- 218 2. Veraverbeke, S. *et al.* Lightning as a major driver of recent large fire years in North
219 American boreal forests. *Nat. Clim. Chang.* **7**, 529–534 (2017).
- 220 3. Calef, M. P., McGuire, A. D. & Chapin, F. S. Human influences on wildfire in Alaska
221 from 1988 through 2005: An analysis of the spatial patterns of human impacts. *Earth*
222 *Interact.* **12**, (2008).
- 223 4. McCarty, J. L., Smith, T. E. L. & Turetsky, M. R. Arctic fires re-emerging. *Nat. Geosci.*
224 **13**, 656–658 (2020).
- 225 5. Irannezhad, M., Liu, J., Ahmadi, B. & Chen, D. The dangers of Arctic zombie wildfires.
226 *Science* (80-.). **369**, 1171 (2020).

- 227 6. Rein, G. Smouldering Fires and Natural Fuels. in *Fire Phenomena and the Earth System:*
228 *An Interdisciplinary Guide to Fire Science* (ed. Belcher, C. M.) 15–34 (2013).
229 doi:10.1002/9781118529539.
- 230 7. Post, E. *et al.* The polar regions in a 2°C warmer world. *Sci. Adv.* **5**, (2019).
- 231 8. Overland, J. E., Wang, M., Walsh, J. E. & Stroeve, J. C. Future Arctic climate changes:
232 Adaptation and mitigation time scales. *Earth's Futur.* **2**, 68–74 (2014).
- 233 9. Tarnocai, C. *et al.* Soil organic carbon pools in the northern circumpolar permafrost
234 region. *Global Biogeochem. Cycles* **23**, 1–11 (2009).
- 235 10. Walker, X. J. *et al.* Increasing wildfires threaten historic carbon sink of boreal forest soils.
236 *Nature* **572**, 520–523 (2019).
- 237 11. Turetsky, M. R. *et al.* Recent acceleration of biomass burning and carbon losses in
238 Alaskan forests and peatlands. *Nat. Geosci.* **4**, 27–31 (2011).
- 239 12. Walker, X. J. *et al.* Soil organic layer combustion in boreal black spruce and jack pine
240 stands of the Northwest Territories, Canada. *Int. J. Wildl. Fire* **27**, 125–134 (2018).
- 241 13. Turetsky, M. R. *et al.* Global vulnerability of peatlands to fire and carbon loss. *Nat.*
242 *Geosci.* **8**, 11–14 (2015).
- 243 14. Flannigan, M. D. *et al.* Fuel moisture sensitivity to temperature and precipitation: climate
244 change implications. *Clim. Change* **134**, 59–71 (2016).
- 245 15. Coops, N. C., Hermosilla, T., Wulder, M. A., White, J. C. & Bolton, D. K. A thirty year,
246 fine-scale, characterization of area burned in Canadian forests shows evidence of
247 regionally increasing trends in the last decade. *PLoS One* **13**, 1–12 (2018).
- 248 16. USDA Forest Service USDI NASF. *Large fire cost reduction action plan.* (2003).
- 249 17. Podur, J. & Wotton, M. Will climate change overwhelm fire management capacity? *Ecol.*

- 250 *Modell*. **221**, 1301–1309 (2010).
- 251 18. Tymstra, C., Stocks, B. J., Cai, X. & Flannigan, M. D. Wildfire management in Canada:
252 Review, challenges and opportunities. *Prog. Disaster Sci.* **5**, 100045 (2020).
- 253 19. Stocks, B. J. *et al.* Large forest fires in Canada, 1959–1997. *J. Geophys. Res.* **108**, (2002).
- 254 20. Wiggins, E. B. *et al.* Evidence for a larger contribution of smoldering combustion to
255 boreal forest fire emissions from tower observations in Alaska. *Atmos. Chem. Phys.*
256 **Preprint**, (2020).
- 257 21. Rein, G., Garcia, J., Simeoni, A., Tihay, V. & Ferrat, L. Smouldering natural fires:
258 Comparison of burning dynamics in boreal peat and Mediterranean humus. *WIT Trans.*
259 *Ecol. Environ.* **119**, 183–192 (2008).
- 260 22. Baber, C. & McMaster, R. *2019 Alaska Statewide Annual Operating Plan. Alaska Master*
261 *Cooperative Wildland Fire Management and Stafford Act Response Agreement Exhibit C*
262 (2019) doi:10.1201/9781315585796-14.
- 263 23. AICC. Wildland Fire Summary and Statistics Annual Report. 1–35 (2010).
- 264 24. Alaska Division of Forestry. State Forestry monitoring hot spots that overwintered from
265 Dëshka Landing Fire. [https://akfireinfo.com/2020/04/10/state-forestry-monitoring-hot-](https://akfireinfo.com/2020/04/10/state-forestry-monitoring-hot-spots-that-overwintered-from-deshka-landing-fire/)
266 [spots-that-overwintered-from-deshka-landing-fire/](https://akfireinfo.com/2020/04/10/state-forestry-monitoring-hot-spots-that-overwintered-from-deshka-landing-fire/) (2020).
- 267 25. Giglio, L., Schroeder, W. & Justice, C. O. The collection 6 MODIS active fire detection
268 algorithm and fire products. *Remote Sens. Environ.* **178**, 31–41 (2016).
- 269 26. Kasischke, E. S., Rupp, T. S. & Verbyla, D. L. Fire trends in the Alaskan boreal forest. in
270 *Alaska's Changing Boreal Forest* (ed. F.S. Chapin, III, M. Oswood, K.V. Cleve, L. A. V.
271 and D. L. V.) 285–301 (Oxford University Press, 2006).
- 272 27. Westerling, A. L., Hidalgo, H. G., Cayan, D. R. & Swetnam, T. W. Warming and earlier

- 273 spring increase Western U.S. forest wildfire activity. *Science* (80-.). **313**, 940–943 (2006).
- 274 28. Painter, T. H. *et al.* Retrieval of subpixel snow covered area, grain size, and albedo from
275 MODIS. *Remote Sens. Environ.* **113**, 868–879 (2009).
- 276 29. Scholten, R. C., Jandt, R. R., Miller, E. A., Rogers, B. M. & Veraverbeke, S. ABoVE:
277 Ignitions, burned area and emissions of fires in AK, YT, and NWT, 2001-2018. (2020)
278 doi:<https://doi.org/10.3334/ORNLDAAAC/1812>.
- 279 30. Xiao, J. & Zhuang, Q. Drought effects on large fire activity in Canadian and Alaskan
280 forests. *Environ. Res. Lett.* **2**, (2007).
- 281 31. Flannigan, M. D. *et al.* Global wildland fire season severity in the 21st century. *For. Ecol.*
282 *Manag.* **294**, 51–64 (2013).
- 283 32. Jolly, W. M. *et al.* Climate-induced variations in global wildfire danger from 1979 to
284 2013. *Nat. Commun.* **6**, 1–11 (2015).
- 285 33. Adams, W. H. *The role of fire in the Alaska taiga. An unsolved problem. Technical report,*
286 *Unpublished report of the Bureau of Land Management, State Office, Anchorage, Alaska,*
287 *USA.* (1974).
- 288 34. Certini, G. Effects of fire on properties of forest soils: A review. *Oecologia* **143**, 1–10
289 (2005).
- 290 35. Kane, E. S., Kasischke, E. S., Valentine, D. W., Turetsky, M. R. & McGuire, A. D.
291 Topographic influences on wildfire consumption of soil organic carbon in interior Alaska:
292 Implications for black carbon accumulation. *J. Geophys. Res. Biogeosciences* **112**, 1–11
293 (2007).
- 294 36. Hoy, E. E., Turetsky, M. R. & Kasischke, E. S. More frequent burning increases
295 vulnerability of Alaskan boreal black spruce forests. *Environ. Res. Lett.* **11**, 1–11 (2016).

- 296 37. Miyanishi, K. & Johnson, E. A. Process and patterns of duff consumption in the
297 mixedwood boreal forest. *Can. J. For. Res.* **32**, 1285–1295 (2002).
- 298 38. Kasischke, E. S. & Turetsky, M. R. Recent changes in the fire regime across the North
299 American boreal region - Spatial and temporal patterns of burning across Canada and
300 Alaska. *Geophys. Res. Lett.* **33**, (2006).
- 301 39. Johnstone, J. F. *et al.* Factors shaping alternate successional trajectories in burned black
302 spruce forests of Alaska. *Ecosphere* **11**, (2020).
- 303 40. Mekonnen, Z. A., Riley, W. J., Randerson, J. T., Grant, R. F. & Rogers, B. M. Expansion
304 of high-latitude deciduous forests driven by interactions between climate warming and
305 fire. *Nat. Plants* **5**, (2019).
- 306 41. Andreae, M. O. & Merlet, P. Emission of trace gases and aerosols from biomass burning.
307 *Global Biogeochem. Cycles* **15**, 955–966 (2001).
- 308 42. Dean, J. F. *et al.* Methane Feedbacks to the Global Climate System in a Warmer World.
309 *Rev. Geophys.* **56**, 207–250 (2018).
- 310 43. Beaudoin, A., Bernier, P. Y., Villemaire, P., Guindon, L. & Guo, X. J. Tracking forest
311 attributes across Canada between 2001 and 2011 using a k nearest neighbors mapping
312 approach applied to MODIS imagery. *Can. J. For. Res.* **48**, 85–93 (2018).

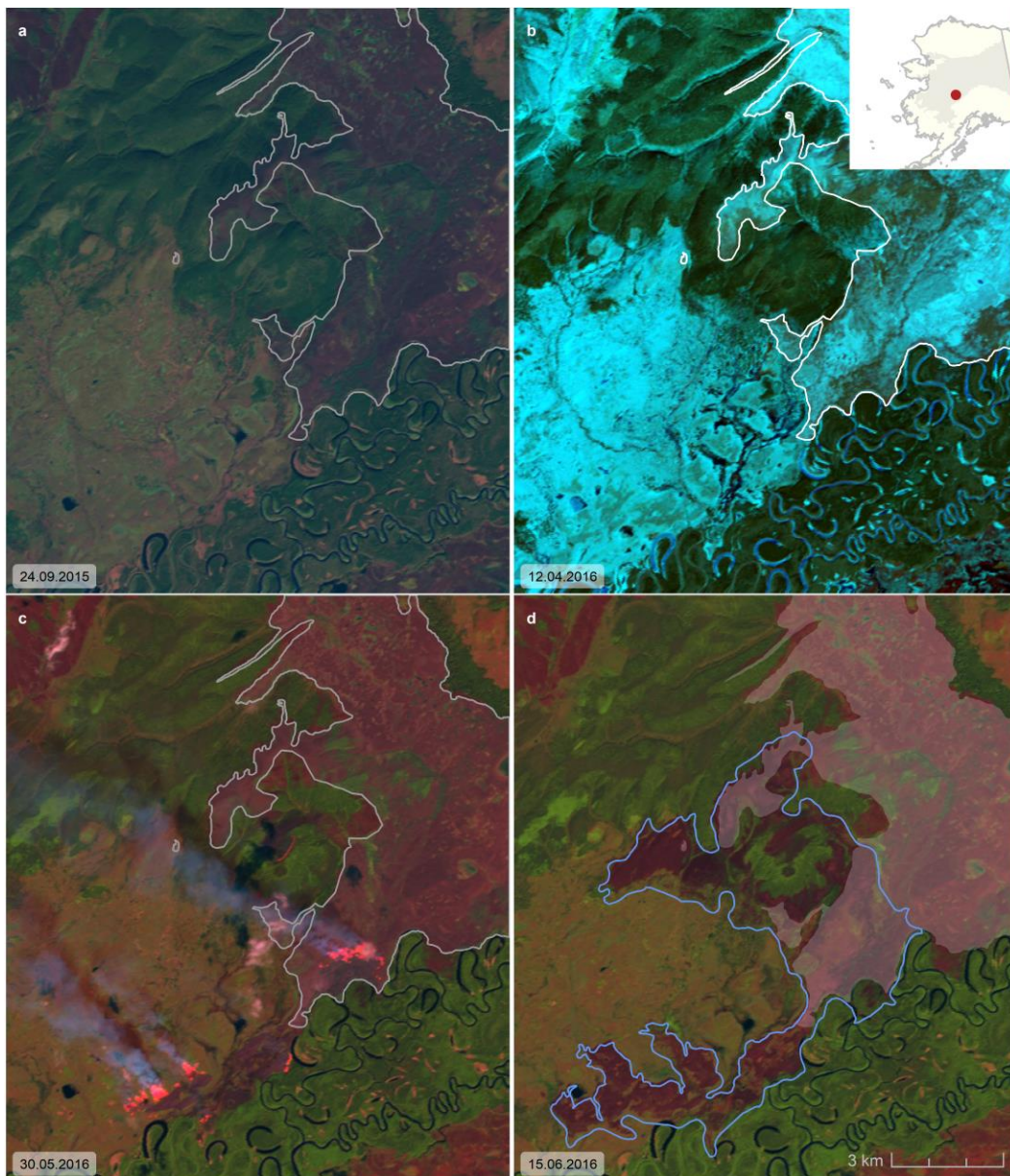
313

314 **Table 1.** Spatial variables differ for fires that produced overwintering fires compared to fires that
 315 did not produce overwintering fires. P-values are based on Welch t-test. Analysis is based on all
 316 (small and large, reported and newly identified) overwintering fires. References for data sources
 317 are given in the methods.

Region	Variable	Source	$\mu_{\text{overwinter}} (\pm \text{S.d.})$	$\mu_{\text{other}} (\pm \text{S.d.})$	p
Alaska			14.0 cm (\pm 3.6)	12.6 cm (\pm 3.3)	0.067
NWT	Burn depth	Alaska Fire Emissions Database v3	16.7 cm (\pm 4.4)	14.1 cm (\pm 3.3)	0.019
Alaska			214.5 m (\pm 149.5)	402.7 m (\pm 358.7)	< 0.001
NWT	Elevation	ArcticDEM	270.5m (\pm 95.4)	356.9 m (\pm 224.0)	0.001
Alaska			2.51° (\pm 2.94)	6.71° (\pm 6.95)	< 0.001
NWT	Slope	ArcticDEM	1.86° (\pm 1.20)	2.90° (\pm 4.08)	0.001
Alaska			0.37 (\pm 0.16)	0.27 (\pm 0.17)	0.001
NWT	Fraction tree cover	MODIS vegetation continuous fields product (MOD44B)	0.23 (\pm 0.09)	0.24 (\pm 0.12)	0.87
Alaska			0.35 (\pm 0.25)	0.25 (\pm 0.23)	0.09
NWT	Fraction black spruce	Fuel Characteristic Classification System Beaudoin et al. (2018) ⁴³	0.28 (\pm 0.17)	0.23 (\pm 0.16)	0.34
Alaska			14.87 kg/m ² (\pm 7.4)	9.5 (\pm 5.1)	0.003
NWT	Organic carbon content in upper (0-30 cm) soil layer	Northern Circumpolar Soil Carbon Database	8.3 kg/m ² (\pm 5.0)	9.3 (\pm 6.1)	0.42

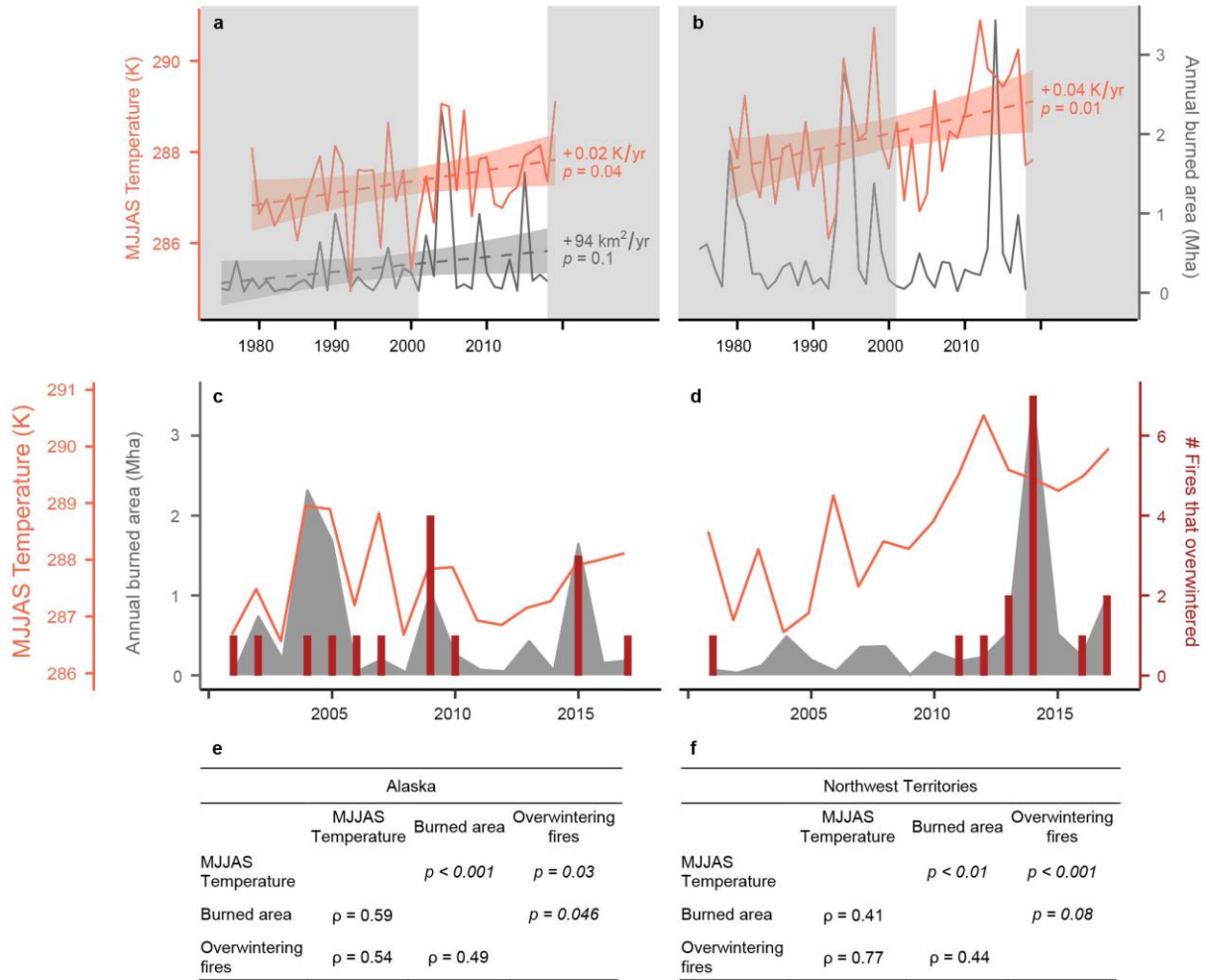
318

319 **Fig. 1.** Landsat 8 false-colour time series of a 2015 fire in Alaska that generated an
320 overwintering fire in 2016. A burn scar at the end of the fire season (white perimeter, A) had
321 seemingly extinguished but was smouldering under the snow layer (B) until favourable
322 conditions enabled the fire to re-emerge (C) thereby creating additional burned area (blue
323 perimeter, D). Fire perimeters were taken from the Alaska Large Fire Database. The Landsat
324 composites used the spectral bands centred at 2.20 μm (red), 0.86 μm (green) and 0.65 μm
325 (blue). Imagery was plotted in R.

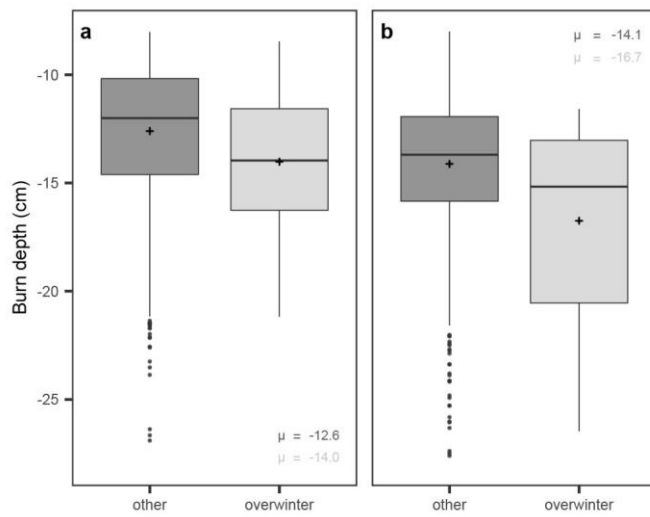


326

327 **Fig. 2.** Temporal drivers of overwintering fires and their long-term trends. Burned area is
328 correlated with the average daily maximum temperature of May – September for Alaska (a, e,
329 Spearman’s $\rho = 0.59, p < 0.001$) and Northwest Territories (b, f, $\rho = 0.41, p < 0.01$), and is
330 increasing in Alaska ($p = 0.10$). May – September maximum temperatures are increasing in
331 Alaska ($p = 0.04$) and Northwest Territories ($p = 0.01$). The number of large overwintering fires
332 correlates with the May – September temperatures in Alaska (e, $\rho = 0.54, p = 0.03$) and
333 Northwest Territories (f, $\rho = 0.77, p < 0.001$), and with burned area from the year in Alaska (c, e,
334 $\rho = 0.49, p = 0.05$) and Northwest Territories (d, f, $\rho = 0.44, p = 0.08$). Large overwintering fires
335 include flare-ups from official reports and additional fires identified by our algorithm. Dashed
336 lines represent significant trends, shaded areas their 95% confidence interval. White areas in a
337 and b refer to the period from 2001 to 2018. Extended Data Figure 6 offers scatterplots of all
338 correlations for visual inspection.

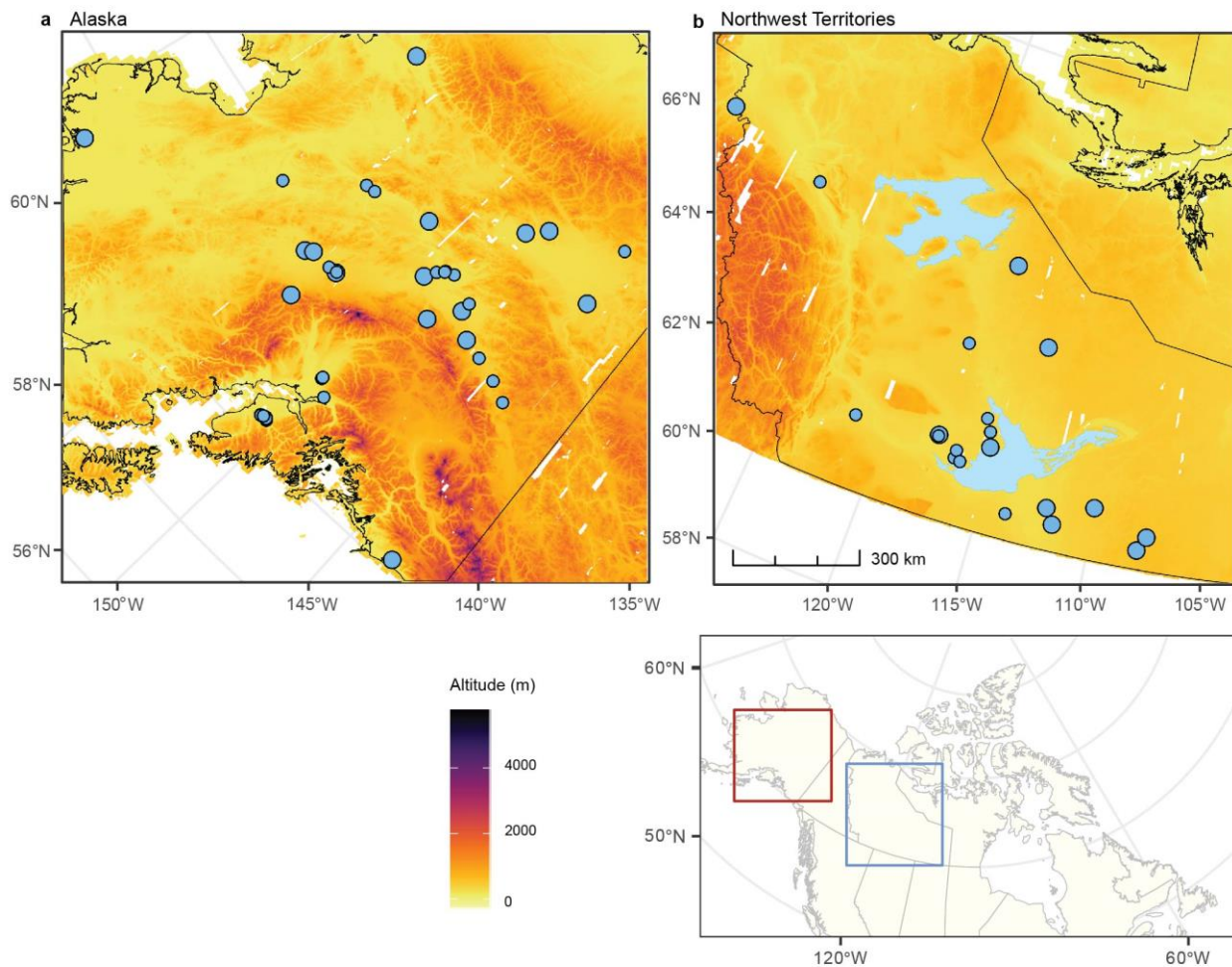


340 **Fig. 3.** Burn scars that generate overwintering fires (light gray) had burned deeper into the soil
341 organic layer compared to fire scars that did not generate overwintering fires (dark gray) in
342 Alaska (a, $p = 0.07$) and Northwest Territories (b, $p = 0.02$). Vertical lines represents the median,
343 plus (+) signs the mean, and lower and upper hinges correspond to 25th and 75th percentiles.
344 Whiskers extend up to 1.5 times the interquartile range, sample points beyond that are
345 represented as dots. We included overwintering fires from government reports and our algorithm.



346

347 **Fig. 4.** Overwintering flare-ups (blue dots) predominantly occur in lowland areas of Alaska (a)
348 and the Northwest Territories (b). Small overwintering fires that were not detected by the
349 Moderate Resolution Imaging Spectroradiometer active fire products are represented as small
350 dots. Large fires (reported and identified by our algorithm) are represented by large dots. White
351 areas represent data gaps in the ArcticDEM. Maps were plotted in R.



352

353 **Methods**

354 **Verified overwintering fires.** Fire managers in Alaska and Canada routinely document
355 information on all fires detected in their territory. These data are assembled in the Alaska Wildland
356 Fire Maps (AWFP; <https://fire.ak.blm.gov/predsvcs/maps.php>) and the Canadian National Fire
357 Database (CNFD)¹⁹. These databases contain the discovery date and location of fires as well as
358 numerous fire attributes such as the size, end date, estimated costs and fire cause. Fire managers
359 attribute ignition causes based on expert knowledge, ground truth or helicopter data, and other
360 sources such as satellite imagery and lightning data. Causes in the fire databases only include
361 human and lightning sources. With rising awareness of overwintering fires, however, some fire
362 managers sparsely started documenting these re-emerging fires in a separate database. We
363 assembled the timing and location of re-emergence of 54 overwintering fires, 42 in Alaska (AK),
364 USA, and 12 in Northwest Territories (NWT), Canada, from these fire management reports. The
365 key characteristics of the overwintering fires used in our study can be found in Supplementary
366 Table 1. Cost data for the fires in Supplementary Tables 1 and 2 were taken from interagency
367 Incident Status Summaries (209 reports) and provided by the Bureau of Land Management, where
368 available, and supplemented by the estimated costs listed in the AWFP database.

369 **Burned area, ignition locations, burn depth and carbon emissions.** We derived the burned area
370 and day of burning for Alaska and Northwest Territories between 2001 to 2018 at 500 m spatial
371 resolution using the Alaskan Fire Emissions Database (AKFED) version 3²⁹, which was updated
372 with input from the Moderate Resolution Imaging Spectroradiometer (MODIS) Collection 6^{2,25}.
373 Daily burned area was retrieved by combining fire perimeter data from the AWFP and the CNFD,
374 and remotely sensed surface reflectance and active fire data from MODIS. After integration of

375 MODIS Collection 6, total burned area and carbon emissions remained within 5 % of previous
376 estimates^{2,44}.

377 The location of the first day of burning of a fire marks the ignition point. We therefore
378 extracted the location and timing of ignitions from local minima within the day of burning variable,
379 denoting the earliest burn date, within each fire perimeter. Fires originating from multiple separate
380 ignitions sometimes grow together in a multi-ignition fire complex. Our algorithm therefore
381 allowed for several ignition points per fire perimeter by using a local minimum search radius of 5
382 km. Although MODIS provides daily coverage of active fires and burned area, the actual ignition
383 location can be obscured if clouds are present, or if a fire starts several hours before the satellite
384 overpass and spreads fast. In these cases, the local minimum contained multiple pixels with the
385 same day of burning. When multiple neighbouring pixels burned at the same day, we estimated
386 the ignition location as the centroid of these pixels and calculated the spatial uncertainty of the
387 ignition locations from the standard deviation in the x and y coordinates of these burned pixels.
388 The spatial standard deviation of the ignition location is as a measure for the ignition location
389 uncertainty. Since the native resolution of the MODIS active fire data is 926.6 m, we added a
390 buffer of 1 km to all ignition locations. For fires with multiple burned pixels on the start date, we
391 extended this 1 km buffer with the spatial standard deviation of the ignition location.

392 Burn depth and emissions were also derived from AKFED version 3, which predicts carbon
393 consumption and burn depth based on remotely sensed pre-fire tree cover, the differenced
394 Normalized Burn Ratio, and temperature and the drought code at the day of burning using a
395 nonlinear multiplicative regression model ($R^2 = 0.39$)². The model was developed using field
396 observations from black spruce (*Picea mariana*) ecosystems. Primary sources of uncertainties that
397 influence the carbon consumption estimate include the unexplained variance in the regression

398 model, the underlying land cover classifications, and consumption scaling for non-black spruce
399 ecosystems. To eliminate uncertainties from consumption scaling in our spatial analysis, we
400 excluded burn scars with high dominance (more than 90 %) of ecosystems other than black spruce.
401 Pixel-level uncertainties in carbon consumption were within 20-25 % of the pixel-level
402 predictions⁴⁴.

403 We used fire perimeter data from CLFD and AAFP to calculate burned area for 1975 to 2000.
404 Since these fire perimeters do not account for unburned islands in the mapped area, we normalised
405 their burned area with AKFED burned area. As in Veraverbeke et al. (2017)², we assumed that
406 uncertainties in fire perimeter mapping have reduced since the integration of Landsat imagery in
407 fire mapping around 1975⁴⁵. The minimum mapping unit (MMU) for the CNFD was 200 ha, and
408 changed over time for AAFP, from 405 ha before 1987 to 40.5 ha between 1987 and 2014, and
409 finally to 4.5 ha starting from 2015. We calculated the ratio of AKFED burned area, which has a
410 MMU of 25 ha, over the ratio of burned area retrieved from the fire perimeters between 2001 and
411 2018. To remove uncertainties due to the MMU, we calculated separate ratios excluding all
412 perimeters smaller than 405 ha and 40.5 for Alaska, and all fires smaller than 200 ha for the
413 Northwest Territories. We multiplied the burned area estimates with the according ratio per region
414 and, in the case for Alaska, time frame. The derived ratios were 0.971 for the Northwest Territories
415 and 0.829 for fires larger than 405 ha, and 0.825 for fires larger than 40.5 ha in Alaska.

416 **Lightning data and lightning ignition attribution.** We acquired data on lightning strikes
417 between 2001 and 2018 detected by the Alaskan Lightning Detection Network (ALDN)⁴⁶ and the
418 Canadian Lightning Detection Network (CLDN)⁴⁷, which contained information on location and
419 timing of cloud-to-ground lightning strikes. The ALDN was started by the Bureau of Land
420 Management Alaska Fire Service (BLM-AFS) in 1976 and has since gradually increased in

421 detection accuracy, efficiency and coverage. The detection accuracy is highest for interior Alaska
422 and decreases towards the coast. A significant upgrade to the system in 2000 led to an increased
423 detection accuracy and efficiency of 0.5 - 2 km and 80 – 90 %, respectively⁴⁶. The replacement of
424 the Impact lightning system with a Time of Arrival (TOA) system in 2012 resulted in a further
425 1.5-fold increase in the detection efficiency, and an increased accuracy stemming from the
426 counting of strokes per flash instead of lightning flashes⁴⁸.

427 Lightning data from the CLDN is available since 1998 and provided by Environment and
428 Climate Change Canada. The CLDN was upgraded gradually, with the largest changes in Northern
429 Canada comprising the addition of two sites in northern Yukon in 2003 and sensor upgrades in
430 NWT and Yukon in 2008 and 2010^{47,49}. For southern NWT, where most of the lightning activity
431 takes place, the CLDN detects approximately 80-90 % of the lightning flashes with a positional
432 accuracy of 500 m⁵⁰. At the periphery of the sensor network, the efficiency decreases to about
433 70 % with positional accuracies between 12 and 22 km. Lightning detection and accuracy
434 decreases to approximately 30 % 300 km beyond the sensor network. Towards north-eastern
435 NWT, accuracy and efficiency markedly decline due to a lack of sensor sites.

436 Between 2001 and 2018, the positional accuracies of the ALDN and CLDN vary substantially
437 in time and space. We therefore adapted a conservative estimate of 2 km for the overall accuracy
438 of the sensor networks and buffered all detected lightning strikes in AK and NWT using this 2 km
439 buffer.

440 We used a spatial and a temporal constraint to assess if an ignition may have been caused by
441 lightning. Both, the ignition locations as well as the lightning locations contain location
442 uncertainties. For the spatial constraint, we thus overlaid all ignition locations including their
443 spatial uncertainty buffer with the buffered lightning strikes of the same year. Subsequently, we

444 compared the date of the lightning strike with the ignition date. Fires often smoulder for several
445 days after a lightning strike before they are detected, yet the lag time between a lightning strike
446 and the ignition detection in boreal forests of North America is not known. Lag times of two or
447 three days have been inferred for fires in Australia, Finland and Florida, U.S.⁵¹⁻⁵³. We extended
448 the lag time threshold to six days to account for longer holdover times that may occur due to the
449 prolonged smouldering in organic soils in boreal North America. Thus, we classified fires with a
450 lightning strike up to six days before the ignition date as started by lightning. We also accounted
451 for a temporal uncertainty of one day in ignition timing⁵⁴. We thereby identified 85 % of the
452 lightning ignitions as reported in the AAFP and CNFD (Extended Data Figure 4A).

453 **Infrastructure data.** We used vector data on roads and other infrastructure elements to assess if
454 an ignition may have been caused by anthropogenic activity. For Alaska, the Alaska Infrastructure
455 1:63,360 shapefile (2006) provided by the Department of Natural Resources comprises all roads
456 and trails, and power and electrical lines. The same infrastructure elements are available from
457 various infrastructure datasets of NWT including the 2010 Road Network File by Statistics
458 Canada⁵⁵ and the Roads 1M dataset by the Government of Yukon⁵⁶, which we combined here.

459 In Alaska, 99 % of ignitions up to 5 km from settlements are human-induced³. We used all
460 fires classified as human-ignited by the AAFP and CNFD to derive a distance threshold from our
461 data. First, we calculated the distance between each ignition point including its uncertainty buffer
462 and its nearest infrastructure element for all ignition points that fell within a distance of 5 km of
463 an infrastructure element. Then, we derived a statistical distribution of these distances for all fires
464 that were classified as human-ignited in the official fire databases. 75 % of the ignitions were
465 within 1 km of an infrastructure element (Extended Data Figure 4B). We therefore classified fires
466 that fell within 1 km of an infrastructure element as human-ignited.

467 **Snow cover data.** We determined the regional first snow-free day of spring between 2001 and
468 2018 from the MODIS daily fractional snow cover product (MODSCAG)²⁸. MODSCAG
469 computes the snow fraction of each 500 m pixel using spectral mixture analysis and has shown to
470 outperform normalized difference snow index-based methods, especially during periods of
471 accumulation and melt⁵⁷. We flagged a pixel as snow-free when its fractional snow cover dropped
472 below 15 %. We determined the period between March 21 (Julian day 80) and July 1 (Julian day
473 182) as spring season and selected the first snow-free day of each pixel during this period. Pixels
474 that were still snow covered by July 1 were flagged as permanent snow cover and excluded from
475 the analysis. We also excluded pixels with persistent missing data due to cloud cover on four or
476 more days preceding the first snow-free day detection. The resulting retrieval contained data for
477 98 % of interior Alaska and 87 % of interior Northwest Territories.

478 For a regional estimate, we calculated the yearly mean of the first snow-free day within the
479 interior boreal regions of Alaska and the Northwest Territories. For Alaska this refers to the
480 intermontane boreal ecoregions between the Brooks Range and the Alaska Range, excluding the
481 coastal Bering ecoregions⁵⁸. For NWT we selected the taiga plains and taiga shield ecozones in
482 Northwest Territories⁵⁹. Only pixels that contained data for all years and had not burned during
483 the 18-year timeframe were included in the regional mean.

484 **Climate and fire weather data.** We extracted meteorological data from North America Regional
485 Reanalysis⁶⁰ (NARR) for our climate analysis. NARR provides climate reanalysis data since 1979
486 at a 32 km resolution based on the NCEP Eta atmospheric model and the Regional Climate Data
487 Assimilation System. We extracted 3-hourly air temperature at 2m, relative humidity, wind speed
488 and precipitation over Alaska and the Northwest Territories, and calculated monthly means of the
489 3-hour period that included local solar noon. We derived vapour pressure deficit (VPD) and fire

490 weather variables following the Canadian Fire Weather Index System (CFWIS)⁶¹ from
491 meteorological variables.

492 **Detection of large overwintering fires.** 45 of the ground-truthed overwintering fires (10 from
493 NWT and 35 from AK, in the following referred to as ‘small fires’) were too small to be detected
494 from the MODIS active fire product that was used within AKFED²⁵ (Supplementary Table 1). We
495 used the spatial and temporal characteristics of these 45 small fires to derive spatial and temporal
496 thresholds for a detection algorithm for larger overwintering fires that can be detected from
497 MODIS imagery. The nine remaining overwintering fires from the fire management reports were
498 large enough to be detected by MODIS and were used as reference data for validation of the
499 detection algorithm (Extended Data Fig. 2).

500 Overwintering fires re-emerge within or in close proximity to burned area from the year
501 before and earlier in the year than the majority of lightning- and human-ignited fires. We calculated
502 the shortest distance between each of the 45 small overwintering fire locations reported by fire
503 managers and any area burned in the previous year based on our burned area product and derived
504 a threshold of 1 km based on the statistical distribution of these distances (Extended Data Figure
505 3) and the spatial resolution of our satellite product. Distributions of the difference between the
506 detection date of the small overwintering fires and the regional snowmelt served for a temporal
507 threshold. We chose a threshold of 48 days, which comprises the 90 % quantile of the distribution.
508 On average, fires are detected by our satellite product within 1.7 days of the discovery date of the
509 fire agencies. We therefore extended the threshold by two days to account for the differences in
510 data sources. We applied both thresholds to all ignitions detected by MODIS between 2002 and
511 2018 to identify potential overwintering fires. From these, we further excluded ignitions that were
512 likely caused by lightning by filtering out all ignitions in spatiotemporal vicinity of a lightning

513 strike. We intersected ignitions and lightning strikes including their spatial uncertainties (2 km for
514 all lightning strikes and the individual positional inaccuracy of each ignition) and allowed for a
515 lag time of six days between lightning strikes and ignition in combination with an uncertainty of
516 one day in the ignition timing. We also excluded ignitions with a likely human origin when these
517 occurred with 1 km of infrastructure, thereby accounting for the spatial uncertainty of the ignitions
518 location.

519 **Uncertainty of our algorithm.** Our estimate of the number of overwintering fires based on these
520 four constraints and moderate resolution satellite data is likely conservative. For the Northwest
521 Territories, for example, some estimates suggest that about one third of all fires in 2015 were
522 caused by overwintering flare-ups⁶². Our algorithm however only classified 4 % of the ignitions
523 to be overwintering fires, although 17.5 % of the ignitions were within a 1 km distance from a
524 previous year fire. Many of these ignitions occurred close to a human infrastructure element or
525 late in the season and were therefore removed by our algorithm to avoid false positives. However,
526 our reference data on overwintering fires suggest that 35 % of the small fires are indeed found
527 within our infrastructure buffer, and emergence dates as late as July have been reported by fire
528 managers.

529 Furthermore, many overwintering fires occur in unburned islands or stay relatively small and
530 are therefore not detected by the MODIS active fire product. The Visible Infrared Imaging
531 Radiometer Suite (VIIRS) active fire detection data product⁶³ has a higher spatial resolution of 375
532 m and is therefore capable of detecting smaller fires. Indeed, using VIIRS data we could detect a
533 further 8 of the 31 overwintering fires that were too small to be detected by MODIS. However,
534 VIIRS data are only available from 2012 onward, which renders it less useful than MODIS for the
535 analysis of longer time periods.

536 **Spatial drivers of overwintering fires.** We extracted burn depth from AKFED for all burn scars.
537 We excluded burn scars with high dominance (more than 90 %) of white spruce, pine and
538 deciduous ecosystems because the burn depth model was developed for black spruce ecosystems.
539 We tested the statistical difference in mean burn depth between burn scars that produced
540 overwintering fires and those that did not using Welch's t-test^{64,65}. We thereby assumed that
541 overwintering fires were caused by the closest fire of the previous year.

542 A variety of datasets were used to analyse additional spatial drivers. The analysis was carried
543 out analogous to the burn depth analysis by comparing the mean over the entire burn scar between
544 fires that produced overwintering fires and those that did not using Welch's t-test. We extracted
545 the elevation and slope for all burn scars from the 100 m resolution ArcticDEM v3.0^{66,67}.
546 ArcticDEM provides high-resolution (up to 2 m) digital surface models of the Arctic from 0.32 to
547 0.5 m resolution panchromatic satellite imagery of the DigitalGlobe collection including
548 WorldView-1 (2007), WorldView-2 (2009), WorldView-3 (2014), and GeoEye-1 (2008)⁶⁸.
549 Annual Terra MODIS Vegetation Continuous Fields Collection 6 data at 250 m resolution
550 (MOD44B)⁶⁹ for the years 2000-2017 were used to derive pre-fire tree cover for each burn scar.
551 Tree species fractions were taken from the Fuel Characteristic Classification System layer of the
552 year 2001⁷⁰⁻⁷² for Alaska, and from^{43,73} for the Northwest Territories. We aggregated the tree
553 species into black spruce (*Picea mariana*), white spruce (*Picea glauca*), deciduous, tundra-grass-
554 shrub and non-vegetated ecosystems, and pine (only present in the Northwest Territories) as
555 described in². Organic carbon content in the upper organic soil layer (0-30 cm depth) was extracted
556 from the Northern Circumpolar Soil Carbon Database⁷⁴.

557 **Temporal drivers of overwintering fires.** We analysed the relationship between the number of
558 overwintering fires, annual burned area and daily maximum temperatures from NARR on a

559 regional scale. Based on scatterplots between all three variables, we chose Spearman correlations
560 because of non-linearity (Extended Data Fig. 6a, b, e), the presence of outliers (Extended Data Fig.
561 6d) and small sample sizes (Extended Data Fig. 6 c-f, n = 17). P-values were computed for all
562 correlations.

563 To analyse the influence of winter and spring weather, we computed Spearman's correlations
564 between overwintering fires and the regional snowmelt, as well as winter and spring temperature,
565 vapour pressure deficit, precipitation and relative humidity. Analogous to the spatial drivers
566 analyses, we also tested for differences in the snowmelt date and fire weather variables in spring
567 between fire scars that facilitated overwintering, and those that did not using Welsh's t-test. For
568 the fire weather variables, we hereby took the average of the 50 days after the average snowmelt
569 of each fire. We further compared vapour pressure deficit and fire weather variables at the day of
570 detection for small and large overwintering fires using Welsh's t-test to assess the influence of
571 spring fire weather on the growth of overwintering fires.

572

573 **References:**

- 574 44. Veraverbeke, S., Rogers, B. M. & Randerson, J. T. Daily burned area and carbon
575 emissions from boreal fires in Alaska. *Biogeosciences Discuss.* **11**, 17579–17629 (2015).
- 576 45. Kasischke, E. S. *et al.* Quantifying burned area for North American forests: Implications
577 for direct reduction of carbon stocks. *J. Geophys. Res. Biogeosciences* **116**, 1–17 (2011).
- 578 46. Farukh, M. A. & Hayasaka, H. Active Forest Fire Occurrences in Severe Lightning Years
579 in Alaska. *J. Nat. Disaster Sci.* **33**, 71–84 (2012).
- 580 47. Burrows, W. R. & Kochtubajda, B. A decade of cloud-to-ground lightning in Canada:
581 1999-2008. Part 1: Flash density and occurrence. *Atmos. - Ocean* **48**, 177–194 (2010).

- 582 48. Bieniek, P. A. *et al.* Lightning Variability in Dynamically Downscaled Simulations of
583 Alaska's Present and Future Summer Climate. *J. Appl. Meteorol. Climatol.* **59**, 1139–1152
584 (2020).
- 585 49. Kochtubajda, B. *et al.* Exceptional cloud-to-ground lightning during an unusually warm
586 summer in Yukon, Canada. *J. Geophys. Res. Atmos.* **116**, 1–20 (2011).
- 587 50. Kochtubajda, B., Stewart, R. & Tropea, B. Lightning and Weather Associated with the
588 Extreme 2014 Wildfire Season in Canada's Northwest Territories. in *24th International*
589 *Lightning Detection Conference* 1–4 (2016).
- 590 51. Dowdy, A. J. & Mills, G. A. Atmospheric and fuel moisture characteristics associated
591 with lightning-attributed fires. *J. Appl. Meteorol. Climatol.* **51**, 2025–2037 (2012).
- 592 52. Larjavaara, M., Pennanen, J. & Tuomi, T. J. Lightning that ignites forest fires in Finland.
593 *Agric. For. Meteorol.* **132**, 171–180 (2005).
- 594 53. Duncan, B. W., Adrian, F. W. & Stolen, E. D. Isolating the lightning ignition regime from
595 a contemporary background fire regime in east-central Florida, USA. *Can. J. For. Res.* **40**,
596 286–297 (2010).
- 597 54. Veraverbeke, S. *et al.* Mapping the daily progression of large wildland fires using MODIS
598 active fire data. *Int. J. Wildl. Fire* **23**, 655–667 (2014).
- 599 55. Statistics Canada. Road Network File 2010.
600 <https://www150.statcan.gc.ca/n1/en/catalogue/92-500-X> (2016).
- 601 56. Government of Yukon. Corporate Spatial Warehouse.
602 ftp://ftp.geomaticsyukon.ca/GeoYukon/Transportation/Roads_1M/ (2018).
- 603 57. Rittger, K., Painter, T. H. & Dozier, J. Assessment of methods for mapping snow cover
604 from MODIS. *Adv. Water Resour.* **51**, 367–380 (2013).

- 605 58. Gallant, A. L., Binnian, E. F., Omernik, J. M. & Shasby, M. B. *Ecoregions of Alaska*.
606 *USGS Professional Paper 1567*. (1995) doi:0160482909r0607010010.
- 607 59. Canadian Council on Ecological Areas (CCEA). Canada Ecozones.
608 <https://www.ccea.org/ecozones-downloads> (2016).
- 609 60. Mesinger, F. *et al.* North American regional reanalysis. *Bull. Am. Meteorol. Soc.* **87**, 343–
610 360 (2006).
- 611 61. Van Wagner, C. E. *Development and structure of the Canadian Fire Weather Index*
612 *System. Forestry Technical Report* vol. 35 (1987).
- 613 62. Alaska Fire Science Consortium. *Opportunities to Apply Remote Sensing in Boreal/Arctic*
614 *Wildfire Management & Science: A Workshop*. (2019).
- 615 63. Schroeder, W., Oliva, P., Giglio, L. & Csiszar, I. A. The New VIIRS 375m active fire
616 detection data product: Algorithm description and initial assessment. *Remote Sens.*
617 *Environ.* **143**, 85–96 (2014).
- 618 64. Welch, B. L. The Significance of the Difference Between Two Means when the
619 Population Variances are Unequal. *Biometrika* **29**, 350–362 (1938).
- 620 65. Welch, B. L. The generalization of ‘Student’s’ problem when several different population
621 variances are involved. *Biometrika* vol. 34 28–35 (1947).
- 622 66. Morin, P. *et al.* ArcticDEM; A Publically Available, High Resolution Elevation Model of
623 the Arctic. *Geophys. Res. Abstr.* **18**, 2016–8396 (2016).
- 624 67. Porter, C. *et al.* ArcticDEM. *Harvard Dataverse* (2018)
625 doi:<https://doi.org/10.7910/DVN/OHHUKH>.
- 626 68. Dai, C., Durand, M., Howat, I. M., Altenau, E. H. & Pavelsky, T. M. Estimating River
627 Surface Elevation From ArcticDEM. *Geophys. Res. Lett.* **45**, 3107–3114 (2018).

- 628 69. Hansen, M. C. *et al.* Global Percent Tree Cover at a Spatial Resolution of 500 Meters:
629 First Results of the MODIS Vegetation Continuous Fields Algorithm. *Earth Interact.* **7**,
630 1–15 (2003).
- 631 70. Pettinari, M. L. & Chuvieco, E. Generation of a global fuel data set using the Fuel
632 Characteristic Classification System. *Biogeosciences* **13**, 2061–2076 (2016).
- 633 71. Ottmar, R. D., Sandberg, D. V, Riccardi, C. L. & Prichard, S. J. An overview of the Fuel
634 Characteristic Classification System - Quantifyin, classifying, and creating fuelbeds for
635 resource planning. *Can. J. For. Res.* **37**, 2383–2393 (2007).
- 636 72. Riccardi, C. L. *et al.* The fuelbed: a key element of the Fuel Characteristic Classification
637 System. *Can. J. For. Res.* **37**, 2394–2412 (2007).
- 638 73. Beaudoin, A., Bernier, P. Y., Villemaire, P., Guindon, L. & Guo, X. . Species
639 composition, forest properties and land cover types across Canada’s forests at 250m
640 resolution for 2001 and 2011. *Nat. Resour. Canada, Can. For. Serv. Laurentian For.*
641 *Centre, Quebec, Canada* (2017) doi:10.23687/ ec9e2659-1c29-4ddb-87a2-6aced147a990.
- 642 74. Hugelius, G. *et al.* The northern circumpolar soil carbon database: Spatially distributed
643 datasets of soil coverage and soil carbon storage in the northern permafrost regions. *Earth*
644 *Syst. Sci. Data* **5**, 3–13 (2013).

645 **Acknowledgments.** We thank the three anonymous reviewers and the editor for their suggestions
646 on the initial manuscript. We would like to thank Cheryl Van Der Horn and Gabriella Branson
647 (Alaska Interagency Coordination Center), and Matthew Coyle (Forest Management Division,
648 Department of Environment and Natural Resources, Government of the Northwest Territories) for
649 providing ground truth data on overwintering fires. We wish to thank Environment and Climate
650 Change Canada for their generous permission to use Canadian Lightning Detection Network data,

651 and the Bureau of Land Management, Alaska Fire Service, for providing cost information. We
652 thank NASA JPL's Snow Data Center for making their MODSCAG data available. This work was
653 funded by the Netherlands Organization for Scientific Research (NWO) through a Vidi grant (Fires
654 Pushing Trees North) awarded to S.V. B.M.R acknowledges support from the National
655 Aeronautics and Space Administration (NASA) Arctic-Boreal Vulnerability Experiment (ABOVE;
656 NNX15AU56A).

657 **Author contributions.** S.V. and R.C.S. designed the research. R.C.S. performed the analysis with
658 input from S.V.. B.M.R. contributed to the interpretation of cost data. R.R.J. and E.A.M.
659 contributed to the interpretation of field data. R.C.S. drafted the manuscript. All authors
660 participated in manuscript editing.

661 **Competing interests.** The authors declare no competing interests.

662 **Data availability.** The location and timing of ignition of the overwintering fires used in this study
663 are found in the Supplementary material. Daily burned area, emissions and ignitions data for
664 Alaska, and the Northwest Territories are archived at the Oak Ridge National Laboratory
665 Distributed Active Archive Center for biogeochemical dynamics
666 (<https://doi.org/10.3334/ORNLDAAAC/1812>). Lightning data is available from the Alaska
667 Interagency Coordination Center (<https://fire.ak.blm.gov/predsvcs/maps.php>) and from
668 Environment and Climate Change Canada. Infrastructure data is available for Alaska from the
669 Department of Natural Resources (<https://catalog.data.gov/dataset/alaska-infrastructure-1-63360>),
670 and for the Northwest Territories from Statistics Canada
671 (<https://www150.statcan.gc.ca/n1/en/catalogue/92-500-X>) and the Government of Yukon
672 (https://hub.arcgis.com/datasets/322b6cf3fa1444c289a1d611a4778ead_42/data). MODSCAG
673 snow fraction data is freely available from the JPL Snow Data Server

674 (<http://snow.jpl.nasa.gov/portal/>). All climate data used in this study is available from the North
675 America Regional Reanalysis (<https://psl.noaa.gov/data/gridded/data.narr.html>). All data used for
676 the analysis of spatial drivers is freely available, including the ArcticDEM
677 (<https://doi.org/10.7910/DVN/OHHUKH>), Northern Circumpolar Soil Carbon Database v2
678 (<https://doi.org/10.5879/ECDS/00000002>) and Fuel Characteristic Classification System
679 (<https://www.landfire.gov/fccs.php>).

680 **Code Availability.** Code used to analyse the data is available from
681 <https://github.com/screbec/Overwintering-fires> or <https://doi.org/10.5281/zenodo.4549321>.

682

Extended Data:

683

Extended Data Fig. 1. Aerial view of the Seven Mile Slough Fire in Alaska on 9 May, 2011.

684

Smouldering hotspots (a) had overwintered and burned in the duff layer below the spruces of an

685

unburned island. Green tree crowns of the fallen trees (b) in the original unburned island (perimeter

686

approximated in black) suggest that tree roots were damaged due to subsurface burning. (Photo by

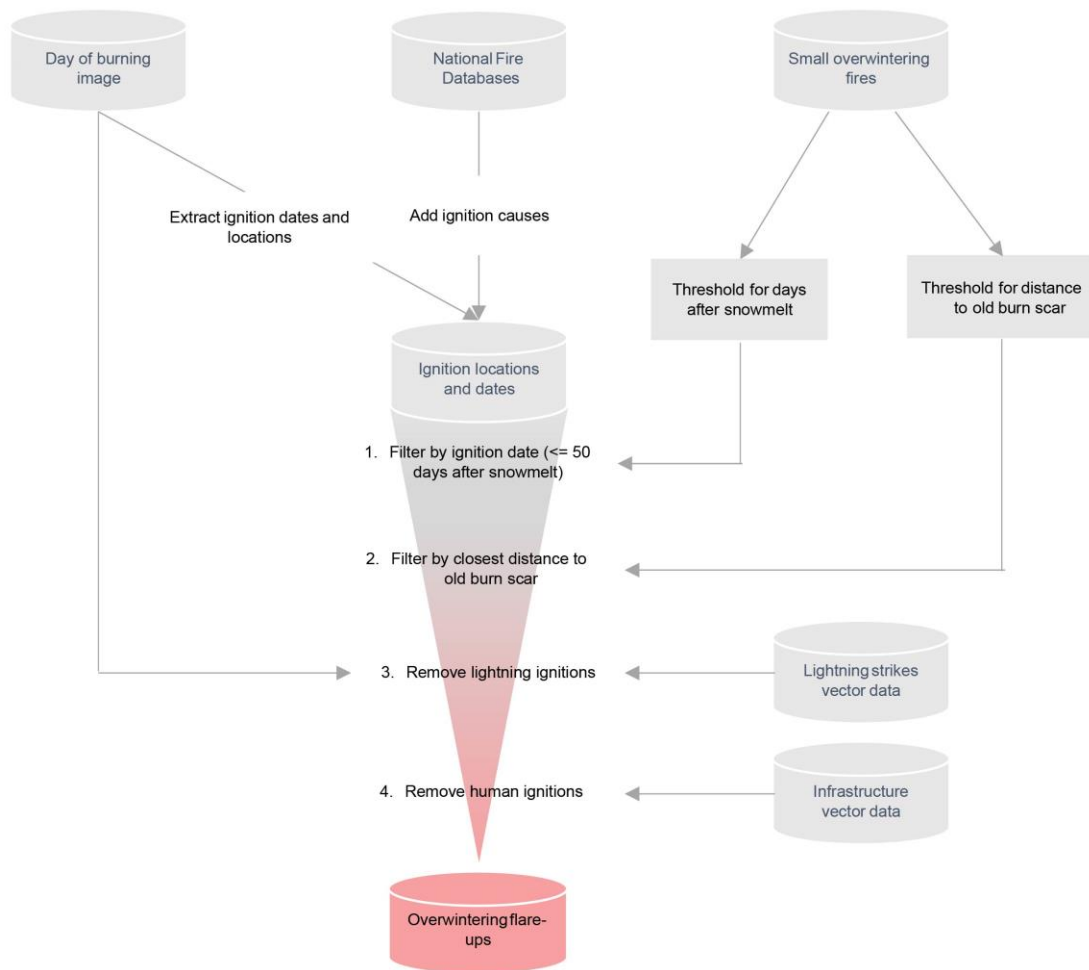
687

Eric Miller)



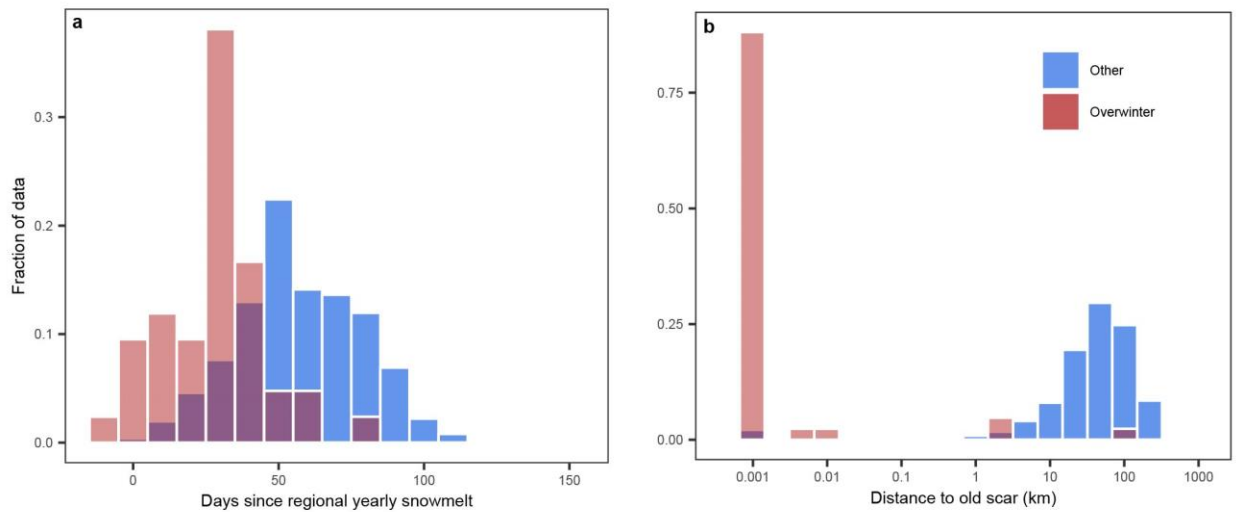
688

689 **Extended Data Fig. 2. Workflow used to detect large overwintering fires.** First, ignition
690 locations, dates, and causes according to official fire databases were extracted. In four steps, the
691 algorithm filters these ignitions by date, distance to an old fire scar, and co-occurrence of
692 lightning strikes and infrastructure elements. Small overwintering fires that were not detected by
693 satellite products were used to derive thresholds for the algorithm.



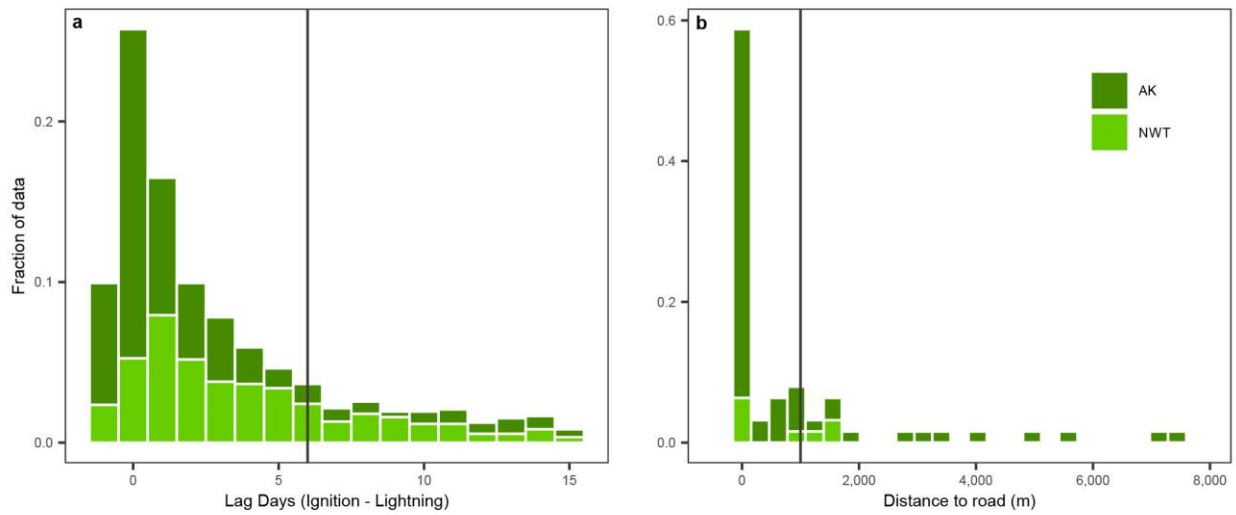
694

695 **Extended Data Fig. 3. Overwintering fires emerge earlier after the seasonal snowmelt (a) and**
 696 **closer to a fire scar from the year before (b) than other fires.** Other fires refer to all fires not
 697 classified as overwintering in official fire databases. Day since regional snowmelt was calculated
 698 from the timing of the ignition points from the Alaskan Fire Emissions Database when possible,
 699 complemented with data from government sources for small fires.



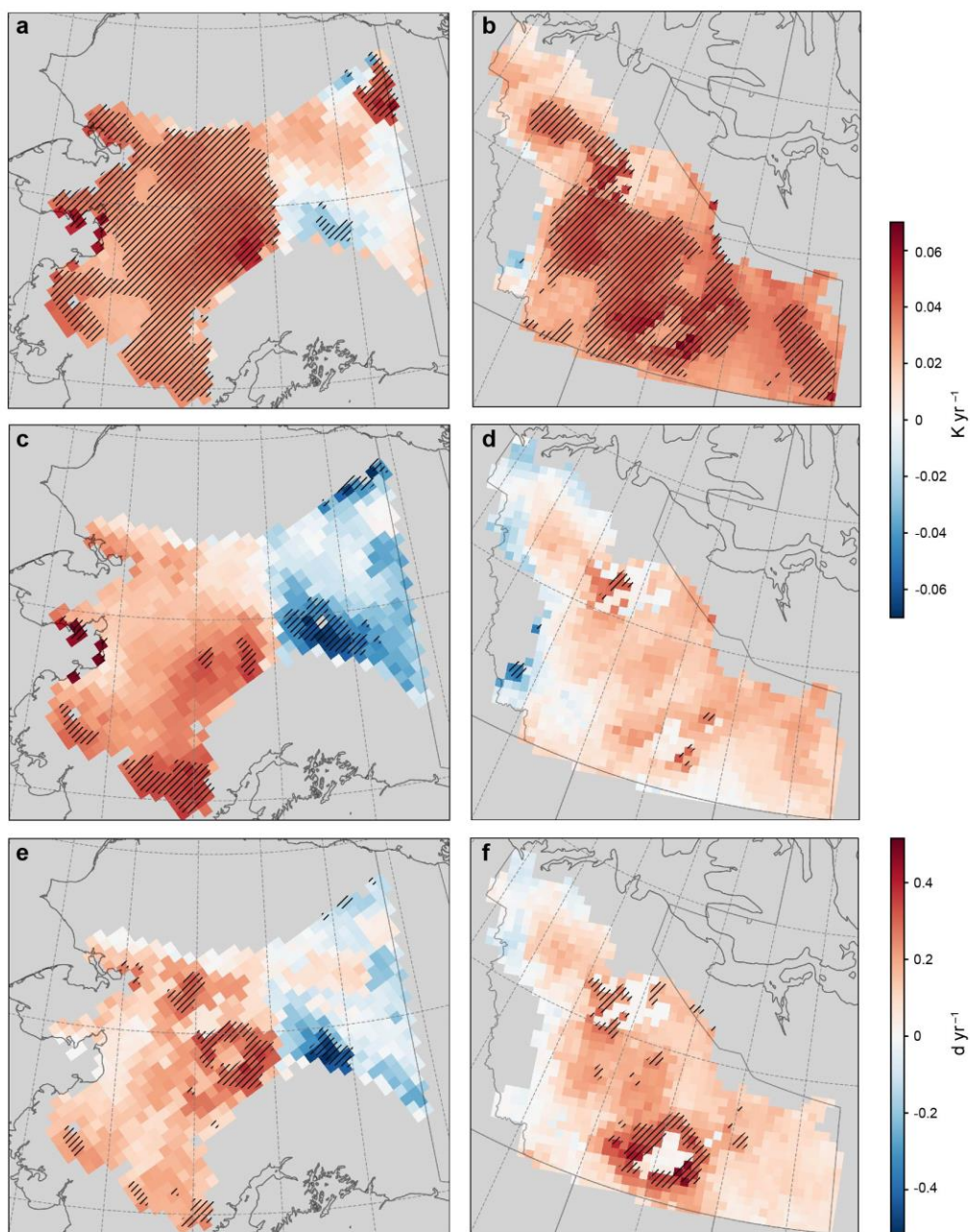
700

701 **Extended Data Fig. 4. Histograms of (a) lag time between lightning strikes and ignition**
702 **detections and (b) distance to road for human ignitions.** Human and lightning ignitions were
703 characterized based on the Alaskan Wildland Fire Maps (AK) and Canadian National Fire
704 Database (NWT). The black lines indicate the thresholds used to eliminate potential overwintering
705 fires due to spatial proximity to infrastructure and spatiotemporal proximity to lightning strikes.



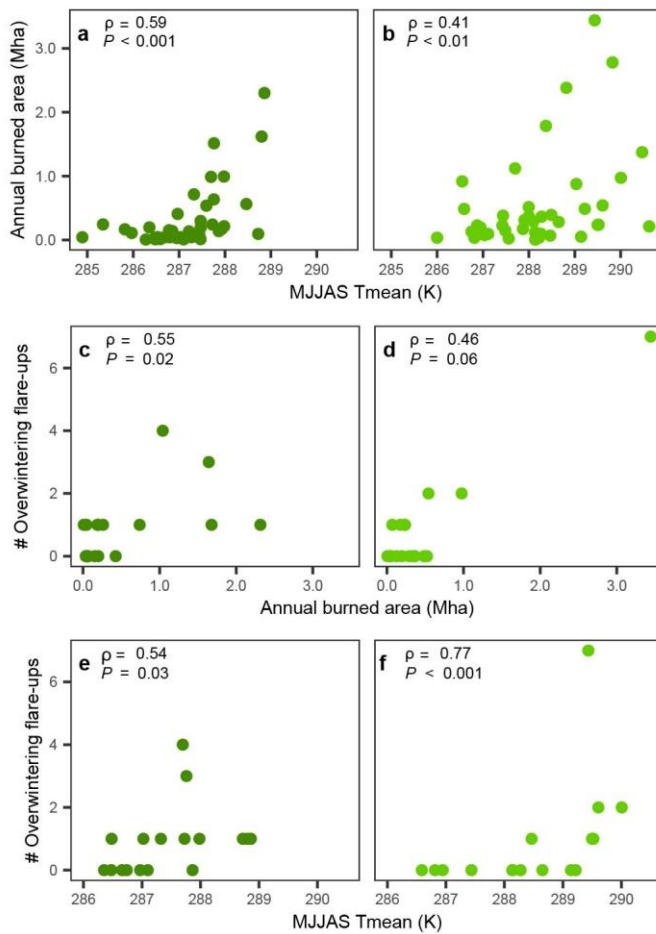
706

707 **Extended Data Fig. 5: Average and extreme temperature trends for interior Alaska and the**
708 **Northwest Territories** a, b, Average of the daily maximum temperature of the summer months
709 May – September. c, d, Its 90th percentile. e, f, Number of hot days surpassing the 90th percentile.
710 Panels a, c, e show data for interior Alaska, and panels b, d, f for the taiga plains and taiga shield
711 of the Northwest Territories.



712

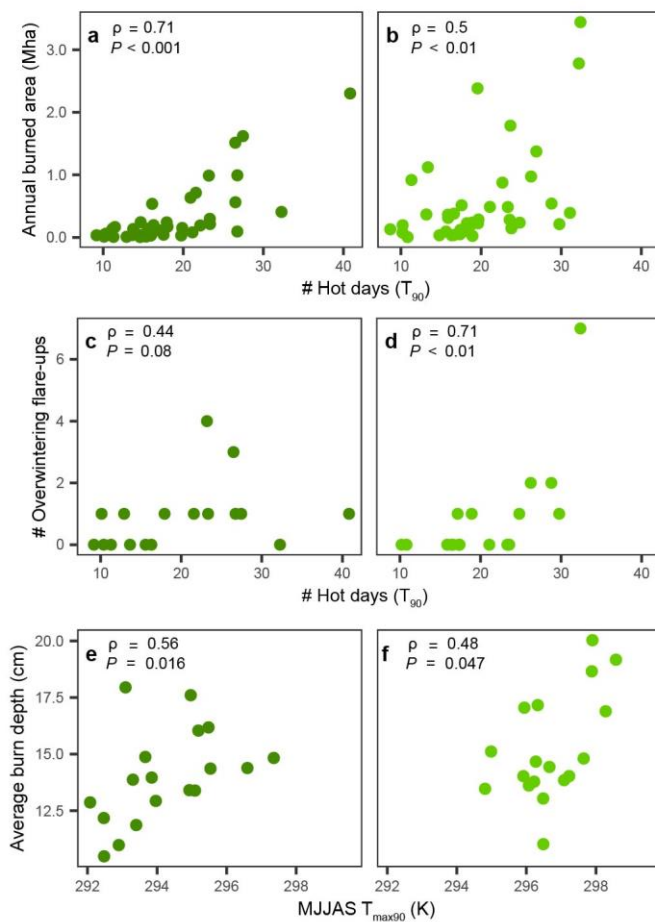
713 **Extended Data Fig. 6: Scatter plots and Spearman correlations of summer temperature,**
 714 **burned area and overwintering flare-ups.** a, b, Daily mean maximum temperature between
 715 May and September (MJJAS) and annual burned area. c, d, Antecedent year's burned area and
 716 the number of overwintering flare-ups. e, f, MJJAS maximum temperature and the number of
 717 overwintering flare-ups. Panels a, c, e show data for Alaska, and panels b, d, f for the Northwest
 718 Territories.



719

720

721 **Extended Data Fig. 7: Scatter plots and Spearman correlations of temperature extremes**
 722 **and burned area, overwintering flare-ups and burn depth.** a, b, Number of MJJAS hot days
 723 (days with a maximum temperature hotter than the 1979-2020 90th percentile) and burned area. c,
 724 d, Number of MJJAS hot days and overwintering ignitions. e, f, 90th percentile of MJJAS
 725 temperature and average burn depth. Panels a, c, e show data for Alaska, and panels b, d, f for
 726 the Northwest Territories.



727

728

Extended Data Tab. 1: Correlation of winter and spring meteorology with the number of

729

overwintering flare-ups in Alaska and Northwest Territories. Results that are significant on a

730

0.1 level are shaded light grey, and those on a 0.05 level dark grey.

Region	Variable	-	Oct	Nov	Dec	Jan	Feb	Mar	Apr	May
Alaska	Regional snow melt	-0.22								
Northwest Territories		-0.06								
Alaska	Average temperature		0.04	0.17	0.05	-0.05	0.16	0.22	0.18	0.08
Northwest Territories			0.37	-0.06	0.08	0.24	0.11	0.29	-0.14	0.22
Alaska	Vapour Pressure Deficit (VPD)		-0.24	-0.07	0.23	-0.08	0.06	0.06	0.1	0.3
Northwest Territories			0.19	-0.07	-0.03	0.21	0.22	0	-0.41	0.37
Alaska	Total precipitation		-0.38	0.06	-0.23	0.13	-0.07	0.08	-0.2	-0.02
Northwest Territories			-0.16	0.28	0.01	-0.09	0.05	0.06	0	-0.08
Alaska	Relative humidity		0.48	0.12	-0.07	0.22	0.06	0.18	-0.31	0.12
Northwest Territories			-0.11	-0.47	0.11	0.21	-0.11	0.04	0.16	0.04

731

732 **Extended Data Tab. 2: Average first snow-free day, vapour pressure deficit (VPD) and**
733 **moisture codes and fire danger indices for days 0 to 50 after the snowmelt did not differ**
734 **significantly for burn scars that produced overwintering fires and those that did not. P-**
735 **values are based on Welch t-test. Analysis is based on all (small and large, reported and newly**
736 **identified) overwintering fires.**

Region	Variable	μ _{overwinter} (± s.d.)	μ _{other} (± s.d.)	<i>p</i>
Alaska	First snow-free day	117.9 (± 13.6)	122 (± 12.3)	0.23
Northwest Territories		128.7 (± 9.3)	130.8 (± 12.5)	0.35
Alaska	Vapour Pressure Deficit (VPD)	836.8 (± 176.2)	804.5 (± 210)	0.45
Northwest Territories		1125.8 (± 295.3)	1115.2 (± 246.8)	0.88
Alaska	Fine Fuel Moisture Code (FFMC)	77.7 (± 5)	76.5 (± 5.6)	0.31
Northwest Territories		81.9 (± 3.8)	80.7 (± 4.7)	0.19
Alaska	Duff Moisture Code (DMC)	21.8 (± 8.2)	21.9 (± 10)	0.97
Northwest Territories		34 (± 13.4)	33.6 (± 13.9)	0.9
Alaska	Drought Code (DC)	121.9 (± 36.6)	134.9 (± 39.7)	0.16
Northwest Territories		166.1 (± 35.7)	172.1 (± 46.5)	0.48
Alaska	Initial Spread Index (ISI)	3.8 (± 1.2)	3.8 (± 1.3)	0.92
Northwest Territories		6.1 (± 1.9)	6 (± 1.8)	0.93
Alaska	Buildup Index (BUI)	14.6 (± 5.2)	14.8 (± 6.6)	0.84
Northwest Territories		22.6 (± 8.4)	23 (± 10.3)	0.84
Alaska	Fire Weather Index (FWI)	5.2 (± 2.3)	5.2 (± 2.7)	0.95
Northwest Territories		9.7 (± 4.1)	9.6 (± 4.2)	0.9
Alaska	Daily Severity Rating (DSR)	0.9 (± 0.6)	0.9 (± 0.7)	0.89
Northwest Territories		2.4 (± 1.4)	2.3 (± 1.6)	0.97

737

738 **Extended Data Tab. 3: Moisture codes and fire danger indices at the day of detection by**
 739 **the AKFED product for overwintering fires smaller and larger than 1 km².** Bold numbers
 740 represent significant differences at $p < 0.1$.

Region	Variable	$\mu_{\text{small}} (\leq 1 \text{ km}^2) (\pm \text{S.d.})$	$\mu_{\text{large}} (> 1 \text{ km}^2) (\pm \text{S.d.})$	p
Alaska	Vapour Pressure Deficit (VPD)	928.7 (\pm 483.6)	1138.4 (\pm 515.3)	0.43
Northwest Territories		1634.2 (\pm 654.7)	1610.7 (\pm 528.8)	0.95
Alaska	Fine Fuel Moisture Code (FFMC)	83.5 (\pm 7.3)	88.2 (\pm 3.8)	0.14
Northwest Territories		84.8 (\pm 6.5)	82.9 (\pm 19.4)	0.68
Alaska	Duff Moisture Code (DMC)	25.3 (\pm 20.0)	34.8 (\pm 19.4)	0.36
Northwest Territories		62.0 (\pm 44.3)	62.8 (\pm 35.7)	0.97
Alaska	Drought Code (DC)	127.4 (\pm 54.4)	156.6 (\pm 41.3)	0.26
Northwest Territories		277.2 (\pm 87.7)	271.3 (\pm 68.7)	0.91
Alaska	Initial Spread Index (ISI)	4.6 (\pm 3.0)	8.7 (\pm 4.1)	0.05
Northwest Territories		7.1 (\pm 5.4)	7.5 (\pm 5.7)	0.90
Alaska	Buildup Index (BUI)	16.4 (\pm 11.6)	22.4 (\pm 11.3)	0.32
Northwest Territories		39.6 (\pm 26.2)	52.5 (\pm 38.6)	0.49
Alaska	Fire Weather Index (FWI)	6.1 (\pm 4.6)	13.2 (\pm 7.3)	0.05
Northwest Territories		15.1 (\pm 14.1)	18.4 (\pm 16.7)	0.71
Alaska	Daily Severity Rating (DSR)	0.9 (\pm 1.0)	3.1 (\pm 2.7)	0.08
Northwest Territories		4.8 (\pm 7.0)	7.1 (\pm 8.6)	0.61

741